Journal of Alloys and Compounds 1044 (2025) 184505

Contents lists available at ScienceDirect

Journal of Alloys and Compounds

journal homepage: www.elsevier.com/locate/jalcom

MetaMode deposition of niobium oxide thin films using a broad-beam ion source

Junwoo Lee [a,*], Yifan Liu [c,e], Carson Malhado [a], Ming Xu [a], Keliang Wang [b], Zhen Qiu [c,d,e,**], Shi-You Ding [f], Richard R. Lunt [a,g], Qi Hua Fan [a,c,***]

[a] Department of Chemical Engineering and Materials Science, Michigan State University, East Lansing, MI, USA
[b] Fraunhofer USA Center Midwest, East Lansing, MI, USA
[c] Department of Electrical and Computer Engineering, Michigan State University, East Lansing, MI, USA
[d] Department of Biomedical Engineering, Michigan State University, East Lansing, MI, USA
[e] Institute for Quantitative Health Science and Engineering, Michigan State University, East Lansing, MI, USA
[f] Department of Plant Biology, Michigan State University, East Lansing, MI, USA
[g] Department of Physics and Astronomy, Michigan State University, East Lansing, MI, USA

ARTICLE INFO

Keywords:
Reactive sputtering
Niobium oxide
Deposition rate
Broad-beam ion source
Optical properties
Surface roughness

ABSTRACT

Niobium oxide (Nb_2O_5) thin films were deposited under MetaMode using a new broad-beam ion source-enhanced magnetron sputtering. The ion source significantly reduced the required oxygen concentration from over 20 % to ~7.5 % to form fully stoichiometric Nb_2O_5 films. The MetaMode deposition rates were over three times higher than conventional reactive magnetron sputtering, which requires significantly higher oxygen concentrations. The film properties were characterized using UV-Vis spectroscopy, atomic force microscopy (AFM), scanning electron microscope (SEM), x-ray diffraction (XRD), x-ray photoelectron spectroscopy (XPS), four-point probe, and spectroscopic ellipsometry. The MetaMode deposited Nb_2O_5 thin films exhibited smoother surfaces, better optical transmittance, and denser morphology, while overcoming the disappearing anode effect in conventional reactive sputtering.

1. Introduction

Niobium pentoxide (Nb_2O_5) thin films exhibit a range of attractive properties that make them suitable for various advanced technological applications. These films typically have a wide bandgap (3.4–4.0 eV), a high refractive index (~2.1–2.4), and a relatively high dielectric constant (20–40), along with excellent optical transparency in the visible and near-infrared regions [1,2]. Depending on the deposition method and thermal treatment, Nb_2O_5 can be amorphous or crystalline, with good thermal and chemical stability [3]. These characteristics make Nb_2O_5 thin films ideal for use in optoelectronic devices, high-κ dielectrics in microelectronics, electrochromic windows, gas sensors, and lithium-ion battery components [4–8]. Additionally, their photocatalytic and nonlinear optical properties open up possibilities for environmental and photonic applications [9–11].

Nb_2O_5 thin films have been fabricated using physical vapor deposition (PVD), chemical vapor deposition (CVD), electron beam evaporation, and sol-gel process [12,13]. Reactive DC sputtering is widely utilized for fabricating oxide films owing to its high throughput and cost-effectiveness [14]. However, this method exhibits several notable limitations when applied to metallic targets. One of the primary challenges is the progressive formation of oxide layers on the target surface, which leads to a significant reduction in the deposition rate, a phenomenon commonly referred to as target poisoning [15]. Another critical yet relatively underexplored issue is the disappearing anode effect, wherein dielectric films deposit on the surrounding anode surfaces (e.g., chamber walls, substrate holders, and target shutters) during reactive sputtering [16–19]. As these surfaces become increasingly insulated, electrons generated in the plasma region encounter difficulty in finding a ground anode, causing unstable discharges [20]. This instability compromises long-term operation and results in poor reproducibility in film properties. One promising approach to addressing

* Corresponding author.
** Corresponding author at: Department of Electrical and Computer Engineering, Michigan State University, East Lansing, MI, USA.
*** Corresponding author at: Department of Chemical Engineering and Materials Science, Michigan State University, East Lansing, MI, USA.
E-mail addresses: leejunw1@msu.edu (J. Lee), qiuzhen@msu.edu (Z. Qiu), qfan@msu.edu (Q.H. Fan).

https://doi.org/10.1016/j.jallcom.2025.184505
Received 21 July 2025; Received in revised form 7 October 2025; Accepted 18 October 2025
Available online 19 October 2025

these limitations is MetaMode sputtering, which decouples the sputtering and film oxidation in two regions. The process repeats the following two sequential steps until achieving the desired film thickness. First, sputter a metal target in a nearly inert gas environment to deposit one to two layers of atoms on a rotating substrate. Second, use a plasma source to oxidize the deposited metal atoms in an oxygen-rich region.

So far, inductively coupled plasma (ICP) sources and gridded ion thrusters have been used for MetaMode sputtering [21–23]. While ICP sources can generate high plasma density, their inherent low ion energy limits the oxidation efficiency, deposition rates, and film packing density [24]. Conversely, gridded ion thrusters can provide higher ion energies but suffer from significant grid erosion over time, curtailing operational longevity [23,25]. Hence, a robust solution to overcome the challenges associated with reactive sputtering deposition of metal oxide thin films remains elusive.

This study introduces an efficient MetaMode sputtering using an innovative broad-beam ion source, which can generate high-density reactive species and simultaneously provide a single broad ion beam with independently controllable ion energy and ion flux. The term *broad-beam* refers to the ion source's ability to produce a wide ion beam (approximately 80 mm in diameter), in contrast to conventional anode-layer ion sources that emit ions through narrow slits of only a few millimeters. Completely stoichiometric Nb_2O_5 films can be formed under nearly metallic sputtering mode. Using lower oxygen concentrations prevents the target poisoning and significantly enhances the deposition rates. While the ion beam focuses on the substrate and fully oxidizes the metal atoms, the materials deposited onto the ground components (e.g., chamber wall and magnetron dark space shield) are still conductive or semi-conductive, alleviating issues related to the disappearing anode effect. This work investigates the effects of oxygen concentrations on Nb_2O_5 thin films deposited with and without the ion source. The studies focus on the optical properties, surface morphology, and electrical resistance of Nb_2O_5 thin films, showing the great potential of MetaMode sputtering to achieve high-rate deposition of high-quality oxide thin films.

2. Experimental details

Nb_2O_5 thin films with a thickness of 100 nm were deposited onto 2.5 cm× 2.5 cm soda-lime glass substrates and p-type (100) silicon wafer of approximately 1 mm thick. Prior to deposition, the substrates were cleaned via ultrasonication sequentially in acetone and deionized (DI) water, followed by drying in an oven at 60 °C for 30 min. The films were deposited using pulsed DC magnetron sputtering assisted by a broad-beam ion source (SPR-100, Scion Plasma LLC) mounted on a top flange of the sputtering system. The magnetron and ion source were positioned at a 45-degree angle, with their axes intersecting at the substrate surface, as illustrated schematically in Fig. 1. The niobium sputtering target, with 99.99 % purity, had a 76.2 mm diameter and 3.2 mm in thickness.

Before the film deposition, the sputtering chamber was evacuated to a base pressure of approximately 2.7×10^{-4} Pa. A pre-sputtering step lasting 15 min was conducted with the substrate shutter closed to remove surface contamination from the target. Depositions were carried out using variable argon-to-oxygen gas ratios, maintaining a deposition pressure of about 0.23 Pa. All the films were deposited at room temperature. The magnetron sputtering power was fixed at 80 W with a pulse frequency of 100 kHz and a reverse pulse duration of 1 ms. The broad-beam ion source can generate ions with a narrowly distributed energy spectrum, while allowing independent control of ion energy and ion flux density within the range of 20–150 eV [26]. In this work, the ion energy of 80 eV was selected. This ion energy is sufficient to oxidize the film and is consistent with our previous studies on the effective ion energy for thin film deposition [26,27]. The ion current was tuned between 200 mA and 425 mA to gauge the effects of ion-surface interactions.

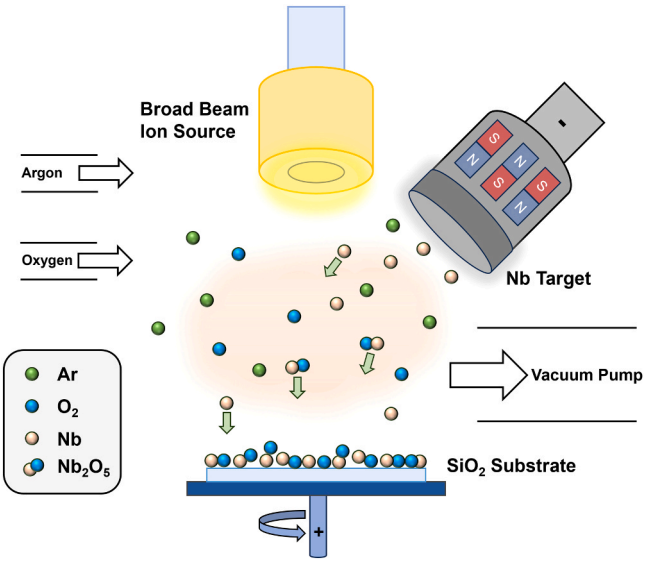

Fig. 1. Schematic drawing of ion source-enhanced reactive sputtering system.

Deposition times were adjusted based on the film growth rates to achieve the targeted film thickness. Film thickness was initially measured with a stylus profilometer (Dektak 150) and confirmed by spectroscopic ellipsometry (M2000, J.A. Woollam). The ellipsometer was also used to determine the film refractive index (n) and extinction coefficient (k) based on a single-layer optical model consisting of a silicon substrate with a Cauchy dispersion layer for fitting. Optical transmittance and reflectance spectra of Nb_2O_5 films were measured using a spectrophotometer (F20, Filmetrics) with a spectral resolution of approximately 1 nm. Surface morphology was assessed by atomic force microscopy (AFM, Bruker Dimension FastScan). Scanning electron microscopy (SEM) was employed to examine the surface morphology using a JSM-7500F. X-ray diffraction (XRD) analysis was performed with a Rigaku Miniflex diffractometer using Cu Kα radiation (λ = 1.54 A). Diffraction patterns were collected over 2θ range of 10° to 60°, with a step size of 0.01° and a scan rate of 10 °/min. Four-point probe (Signatone) was used to measure the sheet resistance of the films. Additionally, X-ray photoelectron spectroscopy (XPS, PHI 5000 VersaProbe II), equipped with a monochromatic Al Kα X-ray source, was utilized to analyze the chemical states of the niobium, collecting high-resolution spectra at a pass energy of 23.5 eV with a step size of 0.1 eV.

3. Results and discussion

3.1. Discharge voltage vs. oxygen concentration in reactive sputtering

Fig. 2 shows the discharge voltage as a function of oxygen (O_2) concentration. The discharge voltage transition occurs between 4 % and 20 % O_2 in sputtering without the ion source, and the transition is reduced to between 4 % and 10 % O_2 in the ion source-enhanced sputtering. The voltage change indicates the transition of the target surface from a metallic state to a compound state, causing reduced secondary electron emissions [28]. The earlier onset of this transition in the ion source-enhanced sputtering implies that the ion source has created additional reactive species, which primarily facilitate the film oxidation and enable a MetaMode deposition of Nb_2O_5 thin films. Additionally, the overall discharge voltage remains lower in the presence of the ion source due to the strongly coupled discharges of the sputtering magnetron and the ion source. It is worth noting that the discharge voltage vs. O_2 concentration relationship is material-specific and depends on the secondary electron emission coefficients of the metal and its oxide. Based on the curves, the films were deposited in two distinct modes marked in Fig. 2. One is the compound mode corresponding to conventional

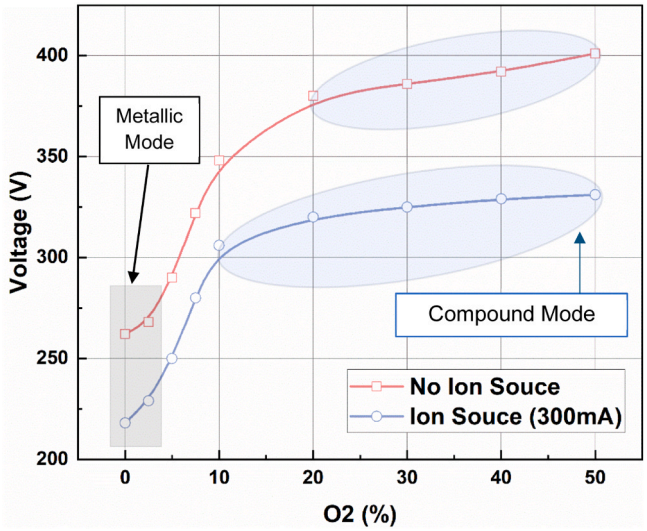

Fig. 2. Variation of discharge voltage as a function of oxygen concentration at a constant pulsed DC sputtering power of 80 W with and without the ion source.

reactive sputtering, under which the oxygen concentration is ~20 % or higher, resulting in nearly fully oxidized target surface and stoichiometry oxide thin films. The other is metallic mode with less than 10 % oxygen concentration, under which the target is only partially oxidized, and the films resulting from conventional reactive sputtering without the ion source consist of a significant fraction of metal atoms.

3.2. Deposition characteristics

Fig. 3 illustrates the deposition rates of niobium oxide thin films with and without the ion source under various O_2 concentrations, demonstrating the film growth rates are highly sensitive to the sputtering atmosphere. In both cases (with and without the ion source), the deposition rates decrease significantly as the O_2 concentration increases from 7.5 % to 20 %. With the ion source, the deposition rate at 7.5 % O_2 is about 4 times higher than that at 20 % O_2; without the ion source, the deposition rate at 7.5 % O_2 is approximately 3 times higher than that at

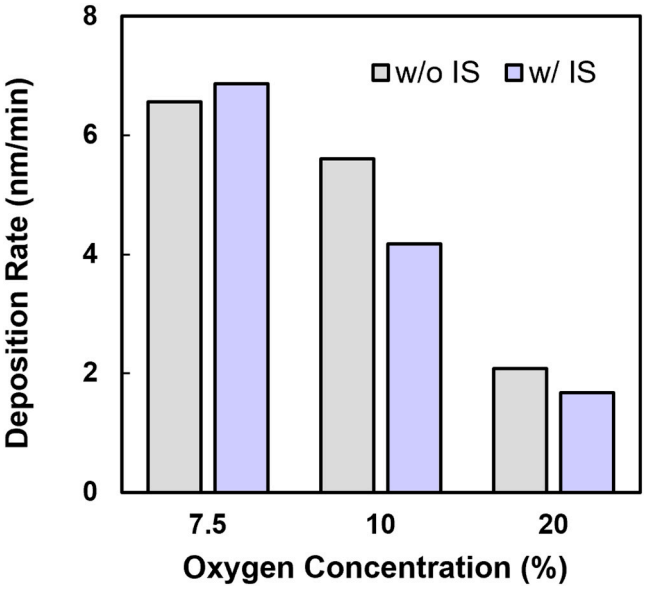

Fig. 3. Deposition rate of niobium oxide thin films without and with ion source (IS) as a function of oxygen concentration, measured at a constant sputtering power of 80 W.

20 % O_2. Hence, change in the deposition rate is more pronounced in ion source-enhanced sputtering than in conventional sputtering without the ion source.

It is well established that as the sputtering target transitions from metallic to compound mode, target poisoning intensifies due to the formation of an insulating oxide layer on the surface. This compound layer has a higher surface binding energy, which reduces the sputtering yield and consequently lowers the deposition rate. The more dramatic decrease in deposition rate in the ion source-enhanced sputtering beyond 7.5 % O_2 can be directly attributed to the discharge voltage behavior discussed previously. For example, at 10 % O_2 concentration, the target surface in the system without ion source remains in the transition region, while the ion source-enhanced sputtering has already reached the compound mode, resulting in much lower sputtering yield.

3.3. Film optical properties

3.3.1. Transmittance and reflectance spectra

Fig. 4 displays the optical transmittance and reflectance spectra of the deposited films in the wavelength range of 400–800 nm, comparing the spectra of films deposited with and without the ion source at three different oxygen gas concentrations: 7.5 %, 10 %, and 20 %.

Fig. 4(a) indicates that the highest optical transmittance, approximately 92.5 %, was achieved in the absence of ion source when the oxygen gas concentration was 20 %. Reducing the oxygen ratio to 10 % and further to 7.5 % led to a progressive decrease in transmittance, respectively. This reduction in transmittance is due to insufficient oxygen levels, which result in incomplete stoichiometric formation of Nb_2O_5, yielding suboxide species adhered to the substrate surface. Such suboxide films, predominantly mixtures of NbO and NbO_2, typically exhibit a surface coloration ranging from gray to light gray [29]. Detailed color comparisons of our films can be found in Fig. S1.

In contrast, as shown in Fig. 4(b), films deposited with ion source exhibited consistently high transmittance, regardless of oxygen concentration. This result suggests that the broad-beam ion source facilitates the formation of fully stoichiometric and optically transparent Nb_2O_5 films, under Meta-Mode sputtering conditions where oxygen supply of 7.5 % is close to metallic mode.

3.3.2. Refractive index n and k

Fig. 5 presents the wavelength-dependent refractive index (n) and extinction coefficient (k) of niobium oxide thin films, measured through ellipsometry analysis across the visible spectrum. Fig. 5 specifically compares n and k numbers of films deposited with and without the assistance of a broad-beam ion source. In the absence of ion source, two distinct oxygen gas concentrations, 7.5 % and 20 %, were selected for comparative analysis. For films deposited with ion source assistance, the oxygen gas concentration was consistently maintained at 7.5 %, while the ion current in the ion source varied among 200 mA, 350 mA, and 425 mA. Table 1 summarizes the n and k values at a representative wavelength of 550 nm for niobium oxide thin films prepared under these varying deposition conditions but maintaining 100 nm of film thickness. The refractive index values ranged from $n = 2.31$ to $n = 2.94$, clearly indicating substantial dependence on deposition conditions.

Notably, the film deposited without ion source assistance at a 7.5 % O_2 displayed a significantly divergent refractive index, $n = 2.94$. For other conditions, the refractive index decreases with increase in wavelength for all prepared films and demonstrates the index values around 2.31, which shows normal dispersion behavior and typical Nb_2O_5 index boundary aligning with other reports [30,31]. In addition, it was found that an increase in ion current slightly increases the index value, highlighting the influence of both the broad-beam ion source and oxygen content on film densification and stoichiometry. The extinction coefficients at 550 nm, also detailed in Table 1, demonstrate that films deposited with ion source assistance exhibit considerably lower k-values ($k < 0.003$), indicative of reduced optical absorption and improved

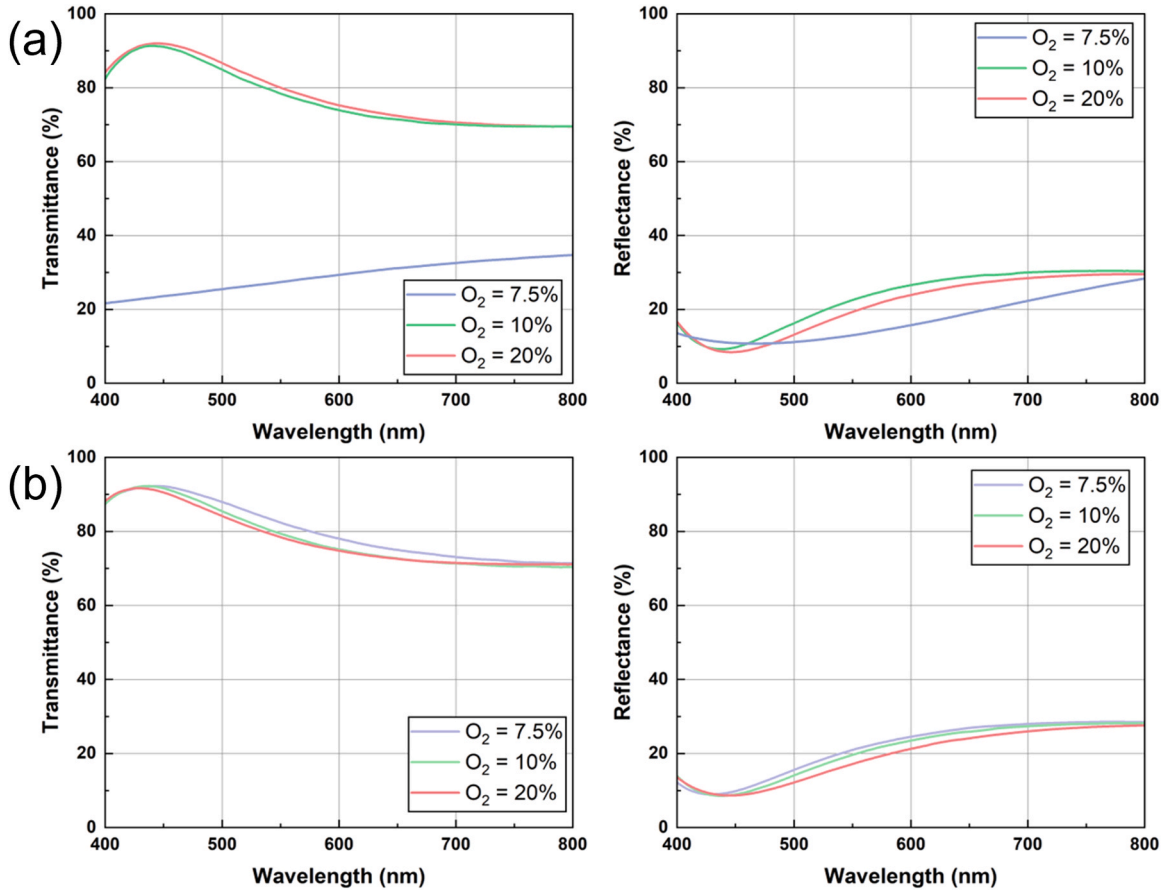

Fig. 4. Transmittance and reflectance of niobium oxide thin films under different deposition conditions: (a) without ion source at varying oxygen concentrations (b) with ion source at varying oxygen concentrations.

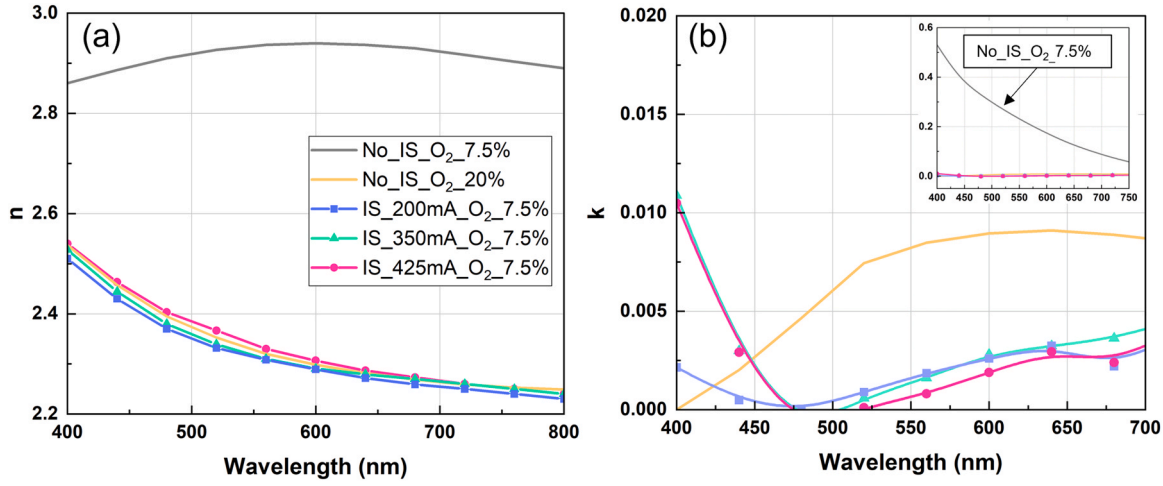

Fig. 5. Refractive index (a) and extinction coefficient (b) of the niobium films deposited under various IS conditions. All films were prepared at a constant sputtering power of 80 W.

transparency. Conversely, the film prepared without the ion source at 7.5 % O_2 exhibited a substantially higher extinction coefficient, $k = 0.23$.

It is also important to highlight that the deviations observed in the refractive index (n) and extinction coefficient (k) at 7.5 % O_2 without ion source assistance are indicative of incomplete oxidation and the presence of sub-stoichiometric or metallic niobium oxide phases. This is primarily due to the insufficient oxygen concentration, which is inadequate to fully oxidize the target surface, as previously discussed in Section 3.2. In particular, it is observed that the extinction coefficient of the film deposited without ion source assistance at 20 % O_2 is higher than that of films fabricated with ion source assistance at 7.5 % O_2. This result can be explained by the limited surface mobility and low kinetic energy of arriving reactive species on substrate surface in the absence of ion bombardment. Without sufficient energy to diffuse across the substrate or occupy low-energy binding sites, atoms are more likely to

Table 1
Refractive index (n) and extinction coefficient (k) of niobium oxide films deposited under various IS conditions measured at a wavelength of 550 nm.

Deposition Condition	Optical properties at 550 nm	
	n	***k***
No_IS_7.5 %	2.94	2.3E−01
No_IS_20 %	2.33	8.50E−03
IS_200mA_7.5 %	2.31	1.70E−03
IS_350mA_7.5 %	2.31	1.40E−03
IS_425mA_7.5 %	2.34	8.70E−04

create loosely packed structures with voids and microstructural inhomogeneities. These voids are a primary source of optical scattering, which elevates the extinction coefficient and degrades the film's optical quality [32,33]. By contrast, the application of ion current and ion energy via the ion source-enhanced sputtering improves atomic mobility through the mechanism of strong atomic peening. The resulting increase in plasma density and ion bombardment improves surface diffusion, allowing atoms to settle into energetically favorable lattice sites and promoting denser niobium oxide films with fewer voids.

3.3.3. Chemical composition of Nb_2O_5 thin films

X-ray photoelectron spectroscopy (XPS) was utilized to evaluate the chemical states of niobium on the surface of niobium oxide thin films deposited by reactive sputtering with and without ion source assistance. The Nb 3d core-level spectra obtained under various deposition conditions are presented in Fig. 6(a). For the films deposited with ion assistance at an oxygen concentration of 7.5 % and without ion source assistance at 20 %, the Nb 3d doublet exhibited a consistent spin-orbit splitting of 2.6 eV, with Nb $3d_{5/2}$ peak positions at approximately 207.15 eV and 207.06 eV, respectively. These peak positions confirm the Nb^{5+} oxidation state, indicative of fully stoichiometric Nb_2O_5 formation [34]. In contrast, the film deposited without ion source assistance at a reduced oxygen concentration of 7.5 % showed a narrower spin-orbit splitting and a Nb $3d_{5/2}$ peak at a lower binding energy of 206.89 eV, suggesting incomplete oxidation and the formation of sub-oxidized niobium species. This XPS result aligns well with the optical properties previously discussed.

In addition, the band gap energy of 3.85–3.9 eV observed for Nb_2O_5 films deposited by ion source-enhanced sputtering, calculated from the Tauc plot (see Fig. S2), further confirms the formation of fully oxidized niobium pentoxide [35]. It is also noteworthy that all the niobium oxides films were deposited at room temperature. The X-ray diffraction (XRD) patterns of Nb_2O_5 thin films (see Fig. 6(b)) displayed amorphous structures, as evidenced by the absence of distinct diffraction peaks. This observation is consistent with other reports stating that niobium oxide films typically remain amorphous when deposited at temperatures below approximately 100°C [34,36].

As shown in Fig. 7, the cross-sectional SEM images reveal no visible crystals in the films, regardless of whether the ion source was employed. The SEM images confirm that, by controlling the deposition parameters and time, consistent film thickness of ~100 nm is achieved.

3.4. Film electrical properties

The sheet resistance of three niobium oxide films was measured using the four-point probe: two samples deposited without the ion source at 7.5 % and 20 % O_2, and one sample fabricated with the ion source at 7.5 % O_2. The sample made without the ion source under 7.5 % O_2 exhibited a semi-conductive behavior with a sheet resistance of approximately 0.4 MΩ. In contrast, the other two samples showed sheet resistances beyond the measurement limit, indicating highly insulating characteristics. These findings suggest, even with only 7.5 % O_2, the ion beam directed to the substrate results in a completely stoichiometric and highly insulating Nb_2O_5 film. On the other hand, films deposited under metallic mode onto the chamber and not subject to the ion beam treatment remain conductive or semi-conductive. This mechanism highlights how the ion source-enhanced sputtering can realize Meta-Mode deposition of metal oxide thin films and mitigate the disappearing anode effect commonly encountered in conventional reactive sputtering.

3.5. Film roughness

In Fig. 8, topological characteristics of 100 nm thickness niobium oxide coated substrates fabricated through the influence of the broad-beam ion source and varying ion source RF powers were evaluated by AFM. It shows a very distinguished and well differentiated surface morphology. Fig. 8(a and d) presents the surface morphology of the film deposited without ion source assistance, which has a sharp columnar structure and exhibits the highest root mean square (RMS) surface roughness of 519.2 sq/pm (as listed in Table 2). In comparison, films deposited with the ion source assistance displayed significantly reduced surface roughness-nearly halving the RMS value. Furthermore, as the ion current in the ion source was increased from 200 eV to 425 eV, a progressive reduction in surface roughness was observed. Across all deposition conditions, the resulting films exhibited crack-free surfaces, affirming the uniformity of the coatings.

These results indicate that the ion source plays a critical role in controlling the roughness of film surfaces. The coarse surface morphology observed in films deposited without the ion source at 7.5 % O_2 is primarily ascribable to the insufficient kinetic energy of arriving species and restricted surface mobility, as previously discussed. The correlation between energy input and surface morphology is well

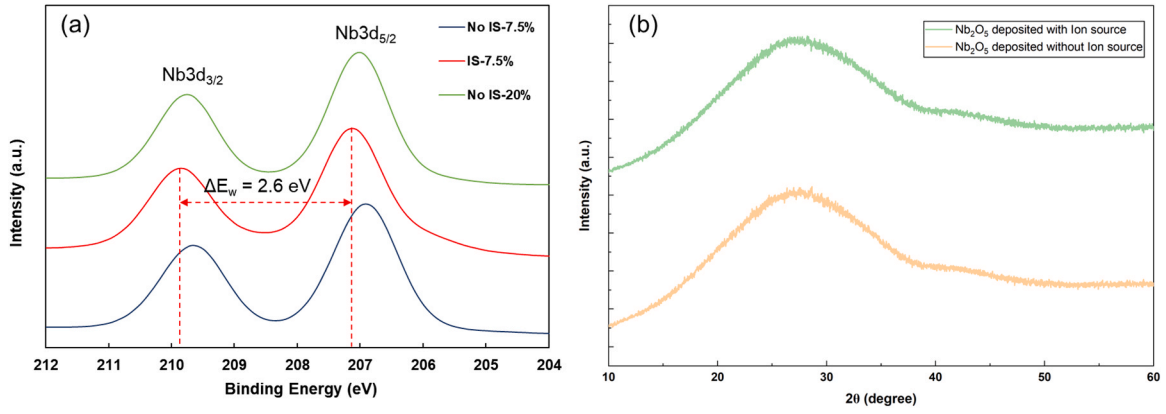

Fig. 6. (a) XPS spectra of Nb 3d core levels from niobium oxide thin films. (b) XRD patterns of a 100 nm-thick niobium oxide film deposited with ion source (green) and without ion source (orange).

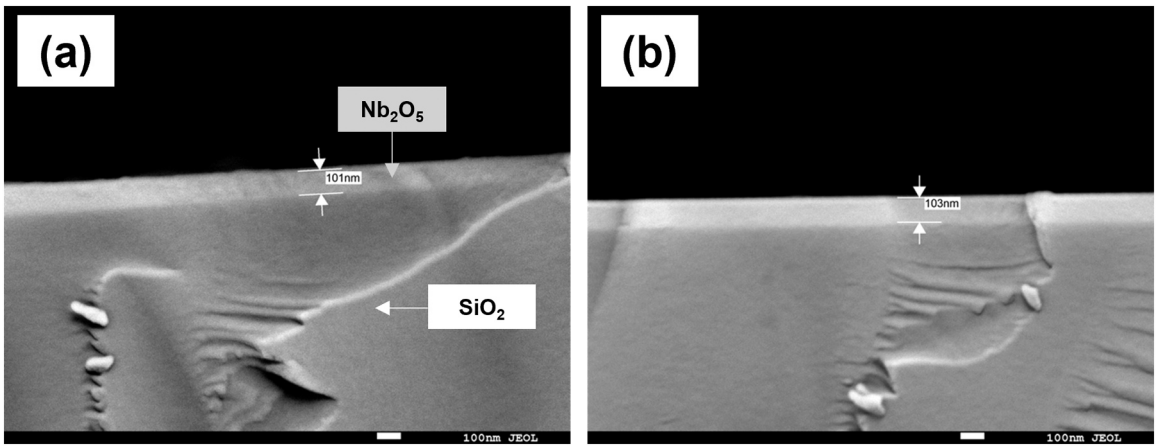

Fig. 7. Cross-sectional SEM of a niobium oxide thin film deposited (a) without ion source and (b) with ion source. Both films were deposited at 7.5 % O_2.

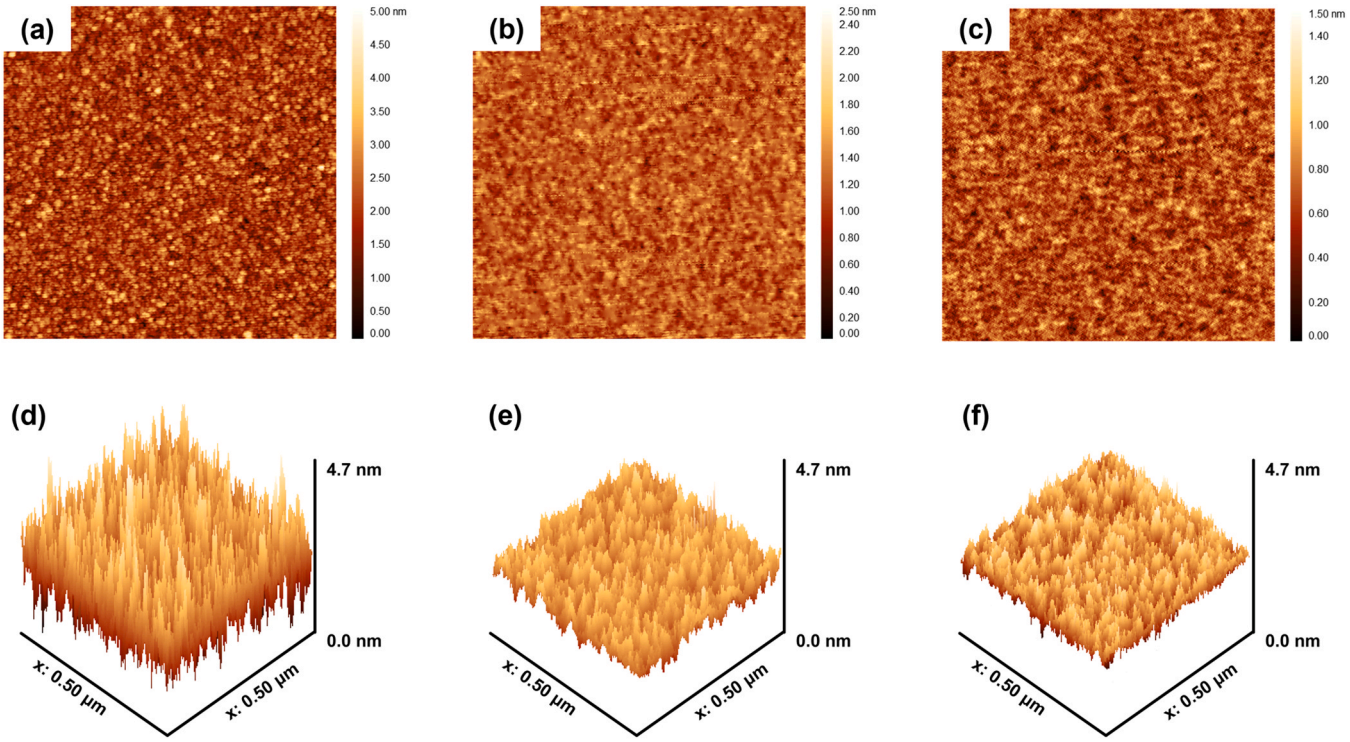

Fig. 8. Surface morphologies of niobium oxide films deposited by ion source-enhanced sputtering, measured by AFM in 2D and 3D under different ion source conditions: (a,d) without ion source; (b,e) with ion source at 200 mA+ 80 eV; and (c,f) with ion source at 350 mA+ 80 eV.

Table 2
Average and RMS roughness of niobium oxide film as a function of different ion source conditions.

Deposition Condition	Average roughness (Sq)/pm	RMS roughness (Sq)/pm
No_IS_O_2_7.5 %	410	519
IS_200mA_O_2_7.5 %	170	214
IS_350 mA_O_2_7.5 %	128	161

supported by the structure zone model [37] and the macroscopic model [38]. At low kinetic energies, sputtered atoms are more prone to gas-phase aggregation, leading to the formation of large atomic clusters or blobs that deposit on the substrate and contribute to rough, columnar surface features [39]. This promotes the growth of prominent large-scale surface undulations rather than smooth and continuous film formation. In contrast, the smoothest surface, obtained at the ion current of 350 mA, is likely due to the closely packed density resulting from enhanced ion bombardment from the use of ion source, which agrees with earlier refractive index observations elucidated in section 3.2.2.

Table 3. exhibits a comparison of the average roughness (R_a) and RMS roughness (R_q) of Nb_2O_5 film from this work with values reported in other studies, all deposited using physical vapor deposition, predominantly magnetron sputtering. It is noteworthy that the films deposited with ion source assistance in this study show among the smoothest surfaces reported to date. Consistent with our observations, several studies that incorporated ion source also demonstrate that film quality, particularly surface roughness, is strongly influenced by ion bombardment and the ion energy.

4. Conclusion

This paper explores the effects of reactive sputtering enhanced by a

Table 3
Average roughness (R_a) and RMS roughness (R_q) of Nb_2O_5 thin films reported.

Film structure (film/substrate)	Deposition method	Thickness, nm	Average roughness (R_a), nm	References
Nb_2O_5 / SiO_2	RF magnetron sputtering	75	2.44	[40]
Nb_2O_5 / Si	Ion-beam sputtering	60	1.5	[41]
Nb_2O_5 / Si	Dual ion assisted sputtering	300	0.97	[42]
Nb_2O_5 / Hard polycarbonate (HPC)	Magnetron ion-assisted deposition	400	0.76	[43]
Nb_2O_5 / Si	Electron beam evaporation	200	0.651	[44]
Nb_2O_5 / SiO_2	Magnetron sputtering	100	0.4	[45]
Nb_2O_5 / Si	Pulsed-DC magnetron sputtering	300	1 (RMS)	[46]
Nb_2O_5 / Si	Ion-assisted reactive magnetron sputtering	100	0.36 (RMS)	[47]
Nb_2O_5 / SiO_2	Pulsed-DC reactive sputtering	100	0.41 (RMS=0.519)	this study
Nb_2O_5 / SiO_2	Ion source-assisted reactive sputtering	100	0.128 (RMS=0.161)	this study

broad-beam ion source on the structural, optical, and morphological properties of niobium oxide thin films. Incorporating an ion source significantly improved the deposition process, allowing for the formation of transparent, fully stoichiometric Nb_2O_5 films with low extinction coefficient at substantially reduced oxygen concentrations compared to conventional reactive sputtering. Importantly, stable MetaMode sputtering was successfully achieved with the ion source, minimizing the formation of undesired suboxide phases. Consequently, the ion source-enhanced sputtering demonstrated deposition rates three to four times higher than those obtained without the ion source. Another key advantage of MetaMode sputtering is its ability to selectively form insulating and semi-conductive oxides: complete oxidation primarily occurs on the substrate surface, while partially oxidized species preferentially deposit onto chamber components, addressing the critical issue of anode insulation. Additionally, higher ion current densifies the film, as evidenced by an elevation in the refractive index from 2.31 to 2.34. The ion source-enhanced sputtering significantly reduced the surface roughness, resulting in approximately 3.2-fold reduction in RMS roughness compared to the films deposited without the ion source. The superior optical properties, coupled with increased deposition rates and reduced roughness, highlight the efficacy of the broad-beam ion source in mitigating the sensitivity to reactive gas inherent in reactive sputtering. This method thus represents a promising advancement for meeting the demands of high-throughput optical coatings manufacturing.

CRediT authorship contribution statement

Junwoo Lee: Writing – original draft, Investigation, Formal analysis, Data curation, Conceptualization. **Qi Hua Fan:** Writing – review & editing, Supervision, Resources, Project administration, Investigation, Conceptualization. **Richard R. Lunt:** Writing – review & editing, Supervision, Resources. **Shi-You Ding:** Resources. **Zhen Qiu:** Supervision, Resources. **Keliang Wang:** Writing – review & editing, Investigation. **Ming Xu:** Investigation. **Carson Malhado:** Writing – review & editing, Investigation. **Yifan Liu:** Investigation, Formal analysis, Data curation.

Declaration of Competing Interest

The authors declare that they have no known competing financial interests or personal relationships that could have appeared to influence the work reported in this paper.

Acknowledgments

This work was supported by the National Science Foundation award number 2243110. Also acknowledged is the MSU TSGTD program.

Appendix A. Supporting information

Supplementary data associated with this article can be found in the online version at doi:10.1016/j.jallcom.2025.184505.

References

[1] M. Vergöhl, B. Hunsche, N. Malkomes, T. Matthée, B. Szyszka, Stabilization of high-deposition-rate reactive magnetron sputtering of oxides by *in situ* spectroscopic ellipsometry and plasma diagnostics, J. Vac. Sci. Technol. A Vac. Surf. Films 18 (4) (2000) 1709–1712, https://doi.org/10.1116/1.582412.
[2] B. Hunsche, M. Vergöhl, H. Neuhäuser, F. Klose, B. Szyszka, T. Matthée, Effect of deposition parameters on optical and mechanical properties of MF- and DC-sputtered Nb2O5 films, Thin Solid Films 392 (2) (2001) 184–190, https://doi.org/10.1016/S0040-6090(01)01025-2.
[3] N. Özer, M.D. Rubin, C.M. Lampert, Optical and electrochemical characteristics of niobium oxide films prepared by sol-gel process and magnetron sputtering a comparison, Sol. Energy Mater. Sol. Cells 40 (4) (1996) 285–296, https://doi.org/10.1016/0927-0248(95)00147-6.
[4] R. Cabanel, J. Chaussy, J. Mazuer, G. Delabouglise, J.C. Joubert, G. Barral, C. Montella, Electrochemichromism of Nb2 o 5 thin films obtained by oxidation of magnetron-sputtered NbN x, J. Electrochem. Soc. 137 (5) (1990) 1444–1451, https://doi.org/10.1149/1.2086688.
[5] F. Lai, L. Lin, Z. Huang, R. Gai, Y. Qu, Effect of thickness on the structure, morphology and optical properties of sputter deposited nb 2 o 5 films, Appl. Surf. Sci. 253 (4) (2006) 1801–1805, https://doi.org/10.1016/j.apsusc.2006.03.014.
[6] K. Kukli, M. Ritala, M. Leskelä, Development of dielectric properties of niobium oxide, tantalum oxide, and aluminum oxide based nanolayered materials, J. Electrochem. Soc. 148 (2) (2001) F35, https://doi.org/10.1149/1.1343106.
[7] M.S. Safavi, F.C. Walsh, L. Visai, J. Khalil-Allafi, Progress in niobium oxide-containing coatings for biomedical applications: a critical review, ACS Omega 7 (11) (2022) 9088–9107, https://doi.org/10.1021/acsomega.2c00440.
[8] Y. Song, T. Sakurai, K. Maruta, A. Matusita, S. Matsumoto, S. Saisho, K. Kikuchi, Opitcal and structural properties of dense SiO2, Ta2O5, and Nb2O5 thin-films deposited by indirectly reactive sputtering technique, Vacuum 59 (2-3) (2000) 755–763, https://doi.org/10.1016/S0042-207X(00)00344-4.
[9] D. Manzani, T. Gualberto, J.M.P. Almeida, M. Montesso, C.R. Mendonça, V.A. G. Rivera, L. De Boni, M. Nalin, S.J.L. Ribeiro, Highly nonlinear Pb2P2O7-Nb2O5 glasses for optical fiber production, J. Non-Cryst. Solids 443 (2016) 82–90, https://doi.org/10.1016/j.jnoncrysol.2016.04.019.
[10] C.L. Ücker, F.C. Riemke, N.F. De Andrade Neto, A.D.A.G. Santiago, T. J. Siebeneichler, N.L.V. Carreño, M.L. Moreira, C.W. Raubach, S. Cava, Influence of Nb2O5 crystal structure on photocatalytic efficiency, Chem. Phys. Lett. 764 (2021) 138271, https://doi.org/10.1016/j.cplett.2020.138271.
[11] K. Su, H. Liu, Z. Gao, P. Fornasiero, F. Wang, Nb2O5-based photocatalysts, Adv. Sci. 8 (8) (2021) 2003156, https://doi.org/10.1002/advs.202003156.
[12] K.-N. Chen, C.-M. Hsu, J. Liu, Y.-C. Liou, C.-F. Yang, Investigation of antireflection Nb2O5 thin films by the sputtering method under different deposition parameters, Micromachines 7 (9) (2016) 151, https://doi.org/10.3390/mi7090151.
[13] K. Yoshimura, T. Miki, S. Iwama, S. Tanemura, Characterization of niobium oxide electrochromic thin films prepared by reactive d.c. Magnetron sputtering, Thin Solid Films 281–282 (1996) 235–238, https://doi.org/10.1016/0040-6090(96)08640-3.
[14] M. Vergöhl, B. Hunsche, N. Malkomes, T. Matthée, B. Szyszka, Stabilization of high-deposition-rate reactive magnetron sputtering of oxides by *in situ* spectroscopic ellipsometry and plasma diagnostics, J. Vac. Sci. Technol. A Vac. Surf. Films 18 (4) (2000) 1709–1712, https://doi.org/10.1116/1.582412.
[15] S. Berg, T. Nyberg, Fundamental understanding and modeling of reactive sputtering processes, Thin Solid Films 476 (2) (2005) 215–230, https://doi.org/10.1016/j.tsf.2004.10.051.
[16] A. Belkind, Z. Zhao, R. Scholl, Dual-anode magnetron sputtering, Surf. Coat. Technol. 163–164 (2003) 695–702, https://doi.org/10.1016/S0257-8972(02)00659-X.
[17] P. Mareš, S. Kadlec, M. Dubau, A. Marek, J. Vyskočil, Long-term stability and disappearing anode effects during reactive DC and pulsed bipolar magnetron sputtering of Al2O3, Vacuum 173 (2020) 109161, https://doi.org/10.1016/j.vacuum.2019.109161.
[18] Segers, A., & Gryse, R.D. (n.d.). Arc Discharges in the Reactive Sputtering of Electrical Insulating Compounds.
[19] J.C. Sellers, The disappearing anode myth: strategies and solutions for reactive PVD from single magnetrons, Surf. Coat. Technol. 94–95 (1997) 184–188, https://doi.org/10.1016/S0257-8972(97)00438-6.

[20] A. Belkind, A. Freilich, G. Song, Z. Zhao, R. Scholl, E. Bixon, Mid-frequency reactive sputtering of dielectrics: Al2O3, Surf. Coat. Technol. 174–175 (2003) 88–93, https://doi.org/10.1016/S0257-8972(03)00369-4.
[21] Carter, D., & McDonough, G. (n.d.). Enhanced Reactively Sputtered Al2O3 Deposition by Addition of Activated Reactive Oxygen.
[22] B. Jorns, T. Lafleur, Foundations of plasmas as ion sources, Plasma Sources Sci. Technol. 32 (1) (2023) 014001, https://doi.org/10.1088/1361-6595/aca560.
[23] T.H. Kim, G.Y. Yeom, A review of inductively coupled plasma-assisted magnetron sputter system, Appl. Sci. Converg. Technol. 28 (5) (2019) 131–138, https://doi.org/10.5757/ASCT.2019.28.5.131.
[24] P.Y. Nabhiraj, R. Menon, G. Mohan Rao, S. Mohan, R.K. Bhandari, Characterization of compact ICP ion source for focused ion beam applications, Nucl. Instrum. Methods Phys. Res. Sect. A Accel. Spectrometers Detect. Assoc. Equip. 621 (1–3) (2010) 57–61, https://doi.org/10.1016/j.nima.2010.04.069.
[25] L. Miao, T. Yang, Z. Zhu, C. Lu, Z. Wu, N. Wang, Status analysis on sputtering and erosion evaluation methods of ion optic systems, Chin. J. Aeronaut. 38 (1) (2025) 103185, https://doi.org/10.1016/j.cja.2024.08.016.
[26] T.A. Amollo, K. Wang, N. Baule, L. Haubold, Q.H. Fan, Hydrogenated diamond-like carbon films grown by a beam plasma source, Diam. Relat. Mater. 154 (2025) 112138, https://doi.org/10.1016/j.diamond.2025.112138.
[27] J. Lee, K. Wang, C. Malhado, Q.H. Fan, Beam plasma source-enhanced deposition of hydrophobic fluorocarbon thin films, Coatings 15 (1) (2025) 110, https://doi.org/10.3390/coatings15010110.
[28] D. Depla, S. Mahieu, R. De Gryse, Magnetron sputter deposition: linking discharge voltage with target properties, Thin Solid Films 517 (9) (2009) 2825–2839, https://doi.org/10.1016/j.tsf.2008.11.108.
[29] R.C. Lee, C.R. Aita, A phase map for sputter deposited niobium oxides, J. Appl. Phys. 70 (4) (1991) 2094–2103, https://doi.org/10.1063/1.349445.
[30] K. Lazarova, B. Georgieva, M. Spasova, T. Babeva, Preparation and characterization of mesoporous Nb_2 O_5 films for sensing applications, J. Phys. Conf. Ser. 558 (2014) 012042, https://doi.org/10.1088/1742-6596/558/1/012042.
[31] Ö.D. Coşkun, S. Demirela, The optical and structural properties of amorphous Nb2O5 thin films prepared by RF magnetron sputtering, Appl. Surf. Sci. 277 (2013) 35–39, https://doi.org/10.1016/j.apsusc.2013.03.116.
[32] Lee, C.-C., Hsu, J.-C., & Wong, D.-H. (n.d.). Low loss niobium oxides ®lm deposited by ion beam sputter deposition.
[33] C.-C. Lee, J.-C. Hsu, D.-H. Wong, The characteristics of some metallic oxides prepared in high vacuum by ion beam sputtering, Appl. Surf. Sci. 171 (1–2) (2001) 151–156, https://doi.org/10.1016/S0169-4332(00)00556-0.
[34] M. Mazur, M. Szymańska, D. Kaczmarek, M. Kalisz, D. Wojcieszak, J. Domaradzki, F. Placido, Determination of optical and mechanical properties of Nb2O5 thin films for solar cells application, Appl. Surf. Sci. 301 (2014) 63–69, https://doi.org/10.1016/j.apsusc.2014.01.144.
[35] E.Z. Kurmaev, A. Moewes, O.G. Bureev, I.A. Nekrasov, V.M. Cherkashenko, M. A. Korotin, D.L. Ederer, Electronic structure of niobium oxides, J. Alloy. Compd. 347 (1–2) (2002) 213–218, https://doi.org/10.1016/S0925-8388(02)00765-X.
[36] X. Liang, B. Liu, Q. Yuan, X. Lin, S. Ren, S. Zhao, X. Yin, S. Fei, Fine control of optical properties of Nb2O5 film by thermal treatment, Micromachines 15 (12) (2024) 1453, https://doi.org/10.3390/mi15121453.
[37] K. Srinivas, M. Manivel Raja, D.V. Sridhara Rao, S.V. Kamat, Effect of sputtering pressure and power on composition, surface roughness, microstructure and magnetic properties of as-deposited Co2FeSi thin films, Thin Solid Films 558 (2014) 349–355, https://doi.org/10.1016/j.tsf.2014.02.052.
[38] G.S. Bales, A. Zangwill, Macroscopic model for columnar growth of amorphous films by sputter deposition, J. Vac. Sci. Technol. A Vac. Surf. Films 9 (1) (1991) 145–149, https://doi.org/10.1116/1.577116.
[39] S.A. Pethe, E. Takahashi, A. Kaul, N.G. Dhere, Effect of sputtering process parameters on film properties of molybdenum back contact, Sol. Energy Mater. Sol. Cells 100 (2012) 1–5, https://doi.org/10.1016/j.solmat.2011.11.038.
[40] K.-N. Chen, C.-M. Hsu, J. Liu, Y.-C. Liou, C.-F. Yang, Investigation of antireflection Nb2O5 thin films by the sputtering method under different deposition parameters, Micromachines 7 (9) (2016) 151, https://doi.org/10.3390/mi7090151.
[41] D.V. Serikov, V.A. Makagonov, S.Yu Pankov, V.A. Dybov, K.S. Gabriels, A. P. Chetverikova, A.A. Polovinkin, Effect of photon treatment on structure of niobium oxide films, AIP Conf. Proc. (2022) 030041, https://doi.org/10.1063/5.0088736.
[42] W. Ai, S. Xiong, Effect of ion bombardment on the properties of Nb2O5 films deposited in large coating chamber, Optik 231 (2021) 166376, https://doi.org/10.1016/j.ijleo.2021.166376.
[43] T.-C. Li, D.-L. Li, J. Ho, C.-C. Yu, S.-S. Wang, J.-J. Ho, Enhancing thickness uniformity of Nb2O5/SiO2 multilayers using shadow masks for flexible color-filtering applications, Micromachines 15 (4) (2024) 551, https://doi.org/10.3390/mi15040551.
[44] J. Han, Y. Lan, Z. Xu, Y. Xu, H. Zhang, Nb2O5 film optical properties and laser-induced damage by phase-change-driven tuning, Ceram. Int. 50 (18) (2024) 32330–32337, https://doi.org/10.1016/j.ceramint.2024.06.040.
[45] X. Liang, B. Liu, Q. Yuan, X. Lin, S. Ren, S. Zhao, X. Yin, S. Fei, Fine control of optical properties of Nb2O5 film by thermal treatment, Micromachines 15 (12) (2024) 1453, https://doi.org/10.3390/mi15121453.
[46] A. Foroughi-Abari, K.C. Cadien, Growth, structure and properties of sputtered niobium oxide thin films, Thin Solid Films 519 (10) (2011) 3068–3073, https://doi.org/10.1016/j.tsf.2010.12.036.
[47] D. You, Y. Jiang, Y. Cao, Y. Zhao, W. Guo, M. Tan, Nb2O5 deposited by ion-assisted reactive magnetron sputtering for near-infrared optical coating: power modulation and performance degradation, Infrared Phys. Technol. 135 (2023) 104978, https://doi.org/10.1016/j.infrared.2023.104978.